

# Block Partitioned Gauss-Seidel PEEC Solver Accelerated by QR-based Coupling Matrix Compression Techniques

Albert Ruehli<sup>††</sup>, Dipanjan Gope<sup>†</sup> and Vikram Jandhyala<sup>†</sup>

<sup>†</sup>Department of Electrical Engineering,  
University of Washington, Seattle 98195.  
{E-mail: dip, jandhyala@ee.washington.edu}

<sup>††</sup>IBM Research Division,  
Yorktown Heights, NY 10598.  
{E-mail: ruehli@us.ibm.com}

## ABSTRACT

*Electromagnetic (EM) integral equation solvers based on the Partial Element Equivalent Circuit (PEEC) approach have proven to be well suited for modeling combined circuit and EM problems. The solution of the full-wave electromagnetic part is transformed to the circuit domain and general well-known circuit solver techniques are applied. However owing to the mutual couplings in the PEEC formulation, the MNA matrix is not sparse as in the case of general lumped circuits. This gives rise to a time and memory bottleneck. In this paper, a Gauss-Seidel relaxation (GSR) solver is presented as an appropriate alternative to SPICE sparse LU solvers, for the PEEC class of problems in the frequency domain. Circuit based block partitioning schemes similar to the ones used in waveform relaxation methods with known convergence properties are used to insure fast convergence. Furthermore, circuit coupling thinning schemes based on QR compression techniques are used to accelerate the inter block updates and also intra block solutions.*

## I. Introduction

The electrical modeling of combined 3D electromagnetic and circuit problems for VLSI systems is ever increasing in complexity and problem size. The PEEC method [1-2] is a popular approach to address these problems using piecewise lumped circuit elements like capacitors, partial inductances, resistors and dependent sources whose values are derived by solving Maxwell's equations on an appropriately discretized 3D mesh. However the MNA matrix for the PEEC class of problems is different from the ones generated for SPICE net-lists consisting of regular lumped circuit elements. In a conventional SPICE circuit formulation using MNA, each node is connected on an average to 4 elements, leading to a sparse matrix system which is ideally solved by a sparse LU solver. Since the integral equation based PEEC formulation includes densely coupled capacitance and inductance sub-matrices, the SPICE type sparse matrix solution [3] is not efficient for these problems.

In existing EM literature several fast Krylov-subspace iterative schemes have been developed to efficiently store and solve the integral equation problem. All these methods including QR-based approaches [4-5], plane-wave expansion methods [6], FFT based techniques [7] etc. accelerate matrix vector products and therefore expedite the iterative process. However, the potential convergence of these iterative solvers depends on the conditioning of the matrix for a particular problem. Further, FFT and plane-wave expansion based approaches are not the best suited for the cases where either PEEC models with high aspect ratio cells are used or when large variations in cell size are involved in the problem.

In this work, we present a block Gauss-Seidel relaxation approach which is based on block partitioning such that convergence in few iterations is guaranteed. The solver has two basic components. First, circuit partitioning based block relaxation schemes similar to the ones used in the waveform relaxation (WR) time domain techniques [8] are employed to come up with an approach where convergence is guaranteed. The partitioning is based on WR circuit coupling criteria as in [9]. Hence, inter-block GSR iterations are performed with guaranteed convergence in few iterations. This is called the outer loop. Secondly, each block is subdivided into hierarchical *sub-blocks*. Each block matrix to be explicitly inverted is thus sparsified and the inter-sub-block GSR iterations are performed. This is termed as the inner loop. The entire process can thus be studied under one outer loop and many intra-block inner loops, as explained in section III. Further, the GSR iterations are expedited by circuit coupling thinning operations based on QR compression which are explained in section IV. The main advantage of the method lies in the guaranteed convergence of the iterative processes. It should also be mentioned here that the circuit coupling thinning percentage achieved through QR-based compression, decays with electrically large structures.

## II. Basic PEEC Cell

The PEEC formulation [1-2] is based on the electric field integral equation:

$$E^i(r_g) = \frac{j}{\sigma} + j\omega A(r_g, r_g') + \nabla\phi(r_g, r_g') \quad (2.1)$$

where  $A$  and  $\phi$  represent the vector and scalar potentials respectively. Using the non-orthogonal local coordinate system [2] and the relations between electric field  $E$  and voltage  $V$  and electric current density  $J$  and electric current  $I$ , (2.1) can be represented with circuit elements. The basic PEEC cell is shown in Fig.1. The number of circuit elements is dominated by the CCVS that model the inductive coupling and the CCCS that model the charge coupling and in Fig. 1 individual dependent sources actually represent series of such elements.

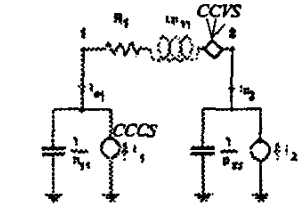


Figure 1: The basic PEEC cell

### III. Gauss-Seidel Iteration Scheme

The main solver presented here is based on the Gauss-Seidel relaxation scheme. The guaranteed convergence for the iterative scheme is heavily dependent on the type of partitioning adopted. In this section we briefly outline the hierarchical *block* (outer loop) and *sub-block* (inner loop) partitioning for the circuit and PEEC parts. Some parts of the circuit and EM problem are strongly connected (SCC) while others are inherently weakly connected (WCC). Similar to [9] we assume that elements form strongly connected components if:

- They share a common node.
- They share a low impedance connection  $Z_c$ , lower than the impedance to the ground.
- The coupling factor between them is smaller than some constant  $\gamma$  which assures fast convergence.

Each PEEC cell has a set of strongly connected component cells e.g. the PEEC cell  $L$  has a strongly connected set:  $L_{SCC} = \{L, M, N, O\}$ . Then a *block* is defined as:  $B = L_{SCC} \cup M_{SCC} \cup N_{SCC} \cup O_{SCC}$ . Hence, elements of a PEEC model for the same body (conductor or dielectric) belong to the same block. If two bodies are connected by SPICE lumped elements, then their PEEC cells belong to the same block if the magnitude of the impedance is smaller compared to the threshold impedance. Otherwise they constitute two separate blocks unless they are extremely close. Also, bodies which are not directly connected will most likely be in different *blocks* since most mutual couplings can be partitioned.

**i) Outer loop:** The entire problem space is first sub-divided into blocks. All the connections and mutual couplings between two blocks must exhibit  $\gamma$  less than a certain value like 0.5 for fast convergence. Therefore the solution is guaranteed to converge at a rate of  $\kappa = O(\gamma^p)$  where  $\kappa$  is the relative error and  $p$  is the number of iterations. Assuming that the system has been divided into 3 blocks, the block matrix system can be written as in (3.1) and the corresponding GS iteration can be performed as in (3.2).

$$\begin{bmatrix} a_{11} & a_{12} & a_{13} \\ a_{21} & a_{22} & a_{23} \\ a_{31} & a_{32} & a_{33} \end{bmatrix} \begin{bmatrix} x_1 \\ x_2 \\ x_3 \end{bmatrix} = \begin{bmatrix} b_1 \\ b_2 \\ b_3 \end{bmatrix} \quad (3.1)$$

$$\begin{cases} x_1 = a_{11}^{-1}(b_1 - a_{12}x_2 - a_{13}x_3) \\ x_2 = a_{22}^{-1}(b_2 - a_{21}x_1 - a_{23}x_3) \\ x_3 = a_{33}^{-1}(b_3 - a_{31}x_1 - a_{32}x_2) \end{cases} \quad (3.2)$$

The inter-block updates in the GSR are expedited by circuit coupling thinning operations as explained in section IV. The main advantage of the block division and the corresponding outer loop lies in the fact that it reduces the size of the matrix that needs to be explicitly inverted.

**ii) Inner loop:** The block matrix inversions shown in (3.2) are again expensive operations owing to the dense nature of the couplings. To alleviate the problem each *block* is further divided into hierarchical spatial *sub-blocks* employing binary decomposition with tight bounds and density balancing to form what is termed as a tight-bound k-d tree. The hierarchical "far" *sub-blocks* are identified and circuit-coupling thinning operations are performed on the mutual couplings between them. These compressed couplings are then extracted out in order to sparsify the matrix to be inverted:  $a_{11} = a_{11}^{close} + a_{11}^{far}$ . The "far" mutual couplings are then updated by a similar GS iterative scheme that is also guaranteed in convergence. If  $b'_1 = b_1 - a_{12}x_2 - a_{13}x_3$  in (3.2), then the iterative process for the inner loop can be written as:

$$x_1 = (a_{11}^{close})^{-1} [b'_1 - a_{11}^{far} x_1] \quad (3.3)$$

On an analysis of the outer and inner loops it can be observed that the matrix to be explicitly inverted is highly sparse and limited in size by block decompositions as shown in Fig. 2.

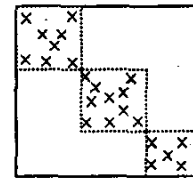


Figure 2: The block sparse matrix to be inverted

#### IV. QR-based Circuit Coupling Thinning

The density in the PEEC model MNA is dominated by the mutual couplings between the inductors and capacitors. In this section we explain how the QR compression technique [4] can be utilized to reduce the number of dependent sources responsible for mutual coupling, which is termed as circuit coupling thinning. Let us consider two well physically separated groups of PEEC inductive cells. We analyze the mutual coupling effects of one group consisting of  $n$  cells (aggressor) on the other group consisting of  $m$  cells. As shown in Fig. 3, the effect can be formulated as current controlled voltage sources (CCVS) associated with every victim inductor. This system of  $m \times n$  CCVS elements can be reduced to fewer circuit elements using the SVD scheme of matrix

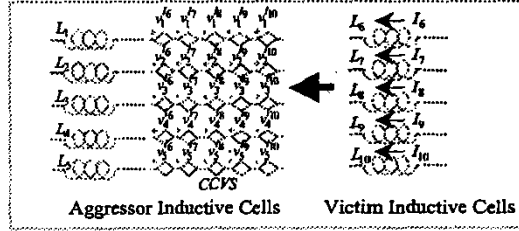


Figure 3: Uncompressed mutual inductive circuit

$$\begin{array}{c}
 \text{CCVS} \quad \text{CCVS} \\
 \begin{bmatrix} v_1^a & v_1^b & v_1^c & v_1^d & v_1^e \\ v_2^a & v_2^b & v_2^c & v_2^d & v_2^e \\ v_3^a & v_3^b & v_3^c & v_3^d & v_3^e \\ v_4^a & v_4^b & v_4^c & v_4^d & v_4^e \\ v_5^a & v_5^b & v_5^c & v_5^d & v_5^e \end{bmatrix} \begin{bmatrix} i_1^a & i_1^b \\ i_2^a & i_2^b \\ i_3^a & i_3^b \\ i_4^a & i_4^b \\ i_5^a & i_5^b \end{bmatrix} \\
 \text{Mutual Matrix} \quad \quad \quad \text{Q} \quad \quad \quad \text{R} \\
 \text{CCCS} \\
 \begin{bmatrix} i_1^a & i_1^b & i_1^c & i_1^d & i_1^e \\ i_2^a & i_2^b & i_2^c & i_2^d & i_2^e \\ i_3^a & i_3^b & i_3^c & i_3^d & i_3^e \\ i_4^a & i_4^b & i_4^c & i_4^d & i_4^e \\ i_5^a & i_5^b & i_5^c & i_5^d & i_5^e \end{bmatrix}
 \end{array}$$

Figure 4: Matrix Perspective

decomposition. Let  $M_{m \times n}$  be the dense matrix representing the CCVS weights. Using a specified tolerance of  $\epsilon = 1e-3$ , this system can be represented as  $M_{m \times n} = U_{m \times r} S_{r \times r} V_{r \times n}$ , where  $r$  is the epsilon-rank of the matrix and  $U$  and  $V$  are orthonormal, which results in every entry of  $U$  and  $V$  being between 0 and 1. Thus the CCVS system can be visualized as in the form of  $[CCVS] = [VCVS] \times [CCVS] \times [CCCS]$ . Intuitively, this is similar to the grouping of source currents into a smaller set ( $r$ ) of currents by CCCS. This small set of

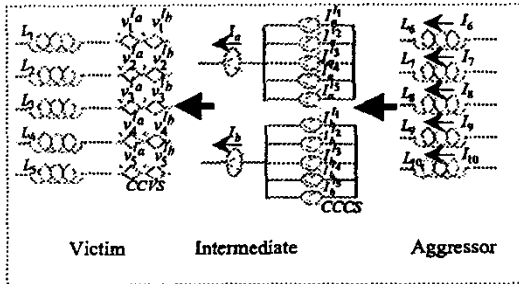


Figure 5: Compressed mutual inductive circuit

currents produces a small set of voltages ( $r$ ) through the CCVS. Finally the small set of voltages is redistributed into the  $m$  voltages by the VCVS. The number of circuit elements can further be reduced by combining the  $[VCVS] \times [CCVS]$  elements directly into CCVS. The SVD method being an expensive process we resort to the modified Gram-Schmidt (MGS) scheme to achieve the same effect as demonstrated in Fig.4. To further simplify the cost of obtaining the reduced set of elements MGS is performed on samples of the  $M_{m \times n}$  matrix [4] thereby achieving the circuit setup in linear time. The final matrix is of the form  $M_{m \times n} = Q_{m \times r} R_{r \times n}$ , where  $R$  is orthonormal. The final circuit structure for the system as shown in Fig. 5, has fewer circuit elements compared to Fig. 3. The fraction of circuit coupling thinning is given by  $\frac{m \times n}{(m+n) \times r}$ . The charge mutual coupling or the CCCS for the capacitors can be similarly treated to reduce the capacitive mutual coupling.

#### V. Numerical Experiments

In this section we provide numerical results to validate the accuracy and time and memory efficiency of the presented scheme. For all cases a QR tolerance of  $1e-3$  and a GS iterative residual of  $1e-3$  were employed. The number of iterations is found to be in the range of 5-10 which is consistent with the maximum coupling factor  $\gamma$  used.

In the first example the accuracy of the solution process is verified. Two conductors are placed as in a transmission line structure as shown in Fig. 6a. Each conductor is of length 50mm and a cross-section of  $20 \mu m \times 1 \mu m$ . The separation between the conductors is  $20 \mu m$ . An ac current source of 1A is connected between the conductors on one end while the other end is connected through a  $500 \Omega$  resistance. This gives rise to a two block problem since the current source is assumed to be infinite impedance. The potential drop across the top

conductor is obtained by a regular SPICE solver and then by the block QR-GSR solver. The results as seen in Fig. 6b and 6c are in good agreement.

In the next example the time and memory efficiencies of the new solver are presented. Figure 7a demonstrates an artificial dielectric structure consisting of two plates at the ends and many conducting bodies in between. Each plate is  $1\ \mu\text{m}$  thick and  $100\ \mu\text{m} \times 100\ \mu\text{m}$  in cross-section. The number of unknowns is increased by increasing the number of conducting objects in the middle. An ac current source of 1A is connected between the plates and the ( $P_n$ )PEEC solver is employed. In Fig. 7b the capacitance is plotted for both solvers and they are found to be in good agreement. It must be noted here that the capacitance value depends on the number of conductors, their shapes and size and their relative placement in between the plates.

In Fig. 7c and 7d the time and memory efficiencies of the QR-GSR solver are demonstrated.

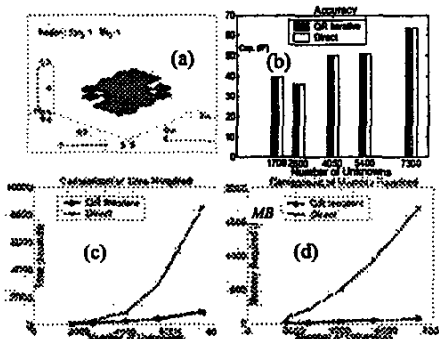


Figure 7: (a) An example of an artificial dielectric structure (b) Accuracy comparison with regular SPICE solver (c) Time comparison with regular SPICE solver (d) Memory comparison with regular SPICE solver

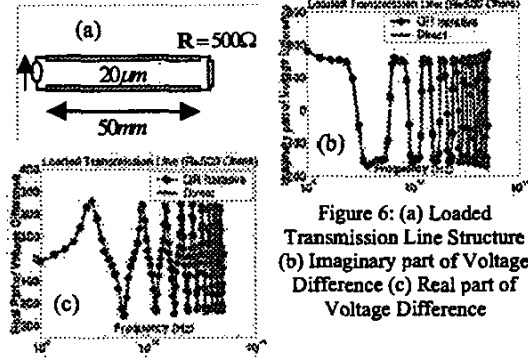


Figure 6: (a) Loaded Transmission Line Structure (b) Imaginary part of Voltage Difference (c) Real part of Voltage Difference

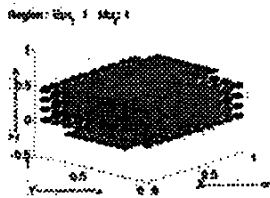


Figure 8: Artificial dielectric with 400 embedded conductors

Unknowns	Memory (MB)	Time (Min)	Cap. (fF)
13,000	666	119	23.99
40,000	1741	344	24.06

Table 1: Time memory and accuracy for different discretizations

In the last example a similar artificial dielectric structure with a  $10 \times 10 \times 4$  array of conductors as shown in Fig. 8, is simulated. The minimum discretization for this problem leads to 13,000 unknowns and higher discretization leads to 40,000 unknowns. The relative time memory and accuracy are shown in Table 1. Both these problems could otherwise not be fitted in the available 2GB memory with the regular sparse LU solver.

## VI. Conclusions

In this paper, a Gauss-Seidel relaxation solver is presented as a more appropriate alternative to the sparse LU SPICE solver. The iterative process is guaranteed in convergence with the adopted partition schemes. Further, the iterations are expedited by the application of circuit coupling thinning techniques based on QR matrix compression.

### References:

- [1] A. E. Ruehli, "Equivalent circuit models for three-dimensional multiconductor systems," *IEEE Trans. on Microwave. Theory and Techniques.*, vol. MTT22 (3), pp. 216-221, March 1974.
- [2] A.E.Ruehli, G.Antonini, J.Esch, J.Ekman, A.Mayo and A.Orlandi, "Nonorthogonal PEEC formulation for time-and frequency-domain EM and circuit modeling", *IEEE Trans. on Electromagnetic Compatibility*, Volume: 45, Issue 2, pp. 167-176, May 2003.
- [3] K. Kundert in A. E. Ruehli, Ed., *Circuit Analysis, Simulation, and Design*, North Holland, Part 1, Elsevier Science Publishing 1986.
- [4] S. Kapur and D. Long, "IES<sup>2</sup>: Efficient Electrostatic and Electromagnetic Simulation," *IEEE Computational Science and Engineering*, vol. 5, no. 4, pp. 60-67, Oct.-Dec. 1997.
- [5] D. Gope and V. Jandhyala, "PILOT: A Fast Algorithm for Enhanced 3D Parasitic Extraction Efficiency", *Proc. IEEE Elec. Perf. of Electronic Packaging conf.*, pp. 337-340, Princeton, NJ, Oct. 2003.
- [6] W.C. Chew, J.M. Jin, E. Michielssen and J. Song, *Fast Efficient Algorithms in Computational Electromagnetics*, Artech House, Boston, London 2001.
- [7] N. Yuan, T.S. Yeo, X.C. Nie and L.W. Li, "A Fast Analysis of Scattering and Radiation of Large Microstrip Antenna Arrays", *IEEE Trans. on Antennas and Propagation*, Vol. 51, Issue 9, pp. 2218-2226, Sep 2003.
- [8] E. Lelarsmeec, A. Ruehli, and A. Sangiovanni-Vincentelli, "The Waveform Relaxation Method for the Time Domain Analysis of Large Scale Integrated Circuits", *IEEE Transactions on Computer-Aided Design for ICs*, pp. 131-145, July 1982.
- [9] J. White and A. L. Sangiovanni-Vincentelli, "Partitioning algorithm and parallel implementations of waveform relaxation algorithms for circuit simulation", *IEEE Proc. Int. Symp. Circuits Syst., ISCAS-85*, pp. 1069-1072, 1985.
- [10] S. Gupta and L.T. Pileggi, "CHIME: Coupled Hierarchical Inductance Model Evaluation", *Proc. IEEE/ACM Design Automation Conference*, pp. 800-805, San Diego, CA, June 2004.